

Velocity and Strain-Rate Profiles in Materials Subjected to Unlubricated Sliding

S. Karthikeyan, H. J. Kim, and D. A. Rigney

Materials Science and Engineering, The Ohio State University, 2041 College Road, Columbus, Ohio 43210, USA

(Received 21 April 2005; published 1 September 2005)

This Letter focuses on the plastic response of a material, treated as a fluid, when subjected to sliding interactions. The analysis couples momentum conservation with material flow laws to predict velocity and strain-rate profiles that develop during sliding. The profiles depend on the strain-rate sensitivity. The spatial extent of the deformed zone is determined by strain-rate sensitivity, strength parameters, and the imposed sliding velocity.

DOI: [10.1103/PhysRevLett.95.106001](https://doi.org/10.1103/PhysRevLett.95.106001)

PACS numbers: 83.50.-v, 46.55.+d, 47.20.Ft

Materials in sliding contact develop large plastic strains and large strain gradients adjacent to the sliding interface. This statement is supported experimentally by observations of surface flow patterns, changes in microstructure, and displacement of markers [1]. Plastic shear strains in the range 10–1000 have been reported [1,2]. Knowledge of strain-rate and strain profiles helps to define not only the region in which most of the deformation occurs, but also the rate of energy dissipation and the friction force. The extent of the plastic zone ranges from the nanoscale to the macroscopic. Flow patterns deduced from marker displacements are similar for a wide range of structures and size scales. These observations suggest that a generic approach, independent of mechanistic deformation details, may be helpful in understanding sliding behavior. A possible approach is to compare the plastic flow of material adjacent to the sliding interface with the response of a fluid when velocity gradients are imposed. Depending on the materials combination and test environment, significant changes in local chemical composition have also been observed. Composition changes are consistent with a mechanism involving mechanical mixing associated with plastic flow [1]. Recent molecular dynamics (MD) simulations reveal the formation of vortices in the vicinity of the sliding interface. It has also been observed that convective material transport and mechanical mixing is most pronounced in the same region where vorticity is highest [1,3,4]. Here again, the situation is reminiscent of fluid flow, for which the well-known Kelvin-Helmholtz instability leads to the formation of eddies [5,6].

This Letter focuses on the response of a block of material when it flows past an identical block with a finite relative velocity. Despite the experimental evidence for developing strain and strain-rate profiles, little work has been done to model these analytically, hence the poor theoretical understanding of friction and flow. This analysis attempts to address this knowledge gap in the area of tribology by applying momentum balance equations and material constitutive laws to predict the velocity profile that develops during sliding. Strain rate is derived from the velocity profile. The uses and limitations of these exact solutions are discussed in the context of plastic deforma-

tion, friction, and microstructure evolution. The broad applicability of the analysis to analogous shearing phenomena, as in shear bands and explosive welding, is also explored.

Two identical materials moving at equal and opposite velocities of $\pm U$ along the x axis are brought into contact (Fig. 1). The flow is one dimensional and symmetric about the flat sliding interface ($y = 0$). Initial conditions are such that the velocity profile $u(y)$ across the interface is a step function. Assuming that the initial interface is infinitely thin, there is an infinite spike in shear strain rate and vorticity at the interface (zero elsewhere). This initial condition is a state of shear instability known as Kelvin-Helmholtz instability [5,6]. This leads to the development of a velocity profile that is a monotonic and continuous function of y and that satisfies the following boundary conditions (BCs): $u = \pm U$ at $y = \pm\infty$; $u = 0$ at $y = 0$ (no slip); $\frac{du}{dy} = 0$ at $y = \pm\infty$.

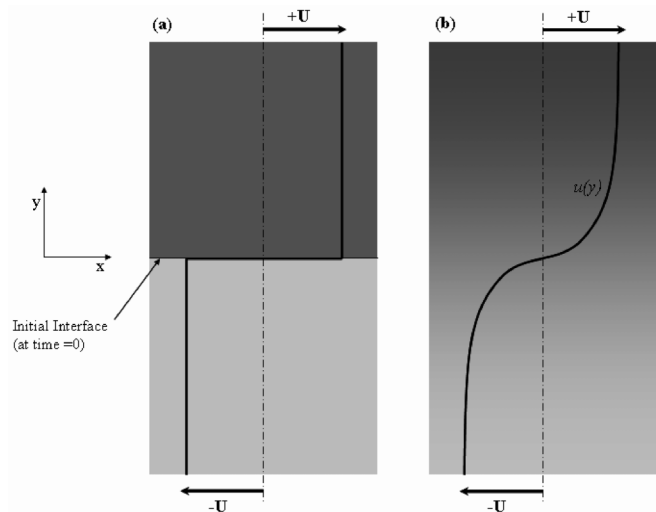


FIG. 1. Schematic showing velocity profile (bold) superimposed on sliding geometry consisting of two semi-infinite blocks. (a) Initially, blocks move rigidly at $\pm U$ with a sharp sliding interface. (b) Later, the interface becomes diffuse and a velocity profile evolves.

Assuming that frictional dissipation is associated primarily with plastic deformation and using variational calculus with the concept of virtual power, it can be demonstrated that the interface spreads and plastic deformation continues to extend into the material. This implies that unless the material is inhomogeneous or softens locally, e.g., via structural and thermal effects, there is no steady-state velocity profile. However, by using a partial differential equation (PDE) to describe local momentum balance and by treating the solid as an incompressible fluid with constant properties, the velocity profile can be calculated. In the absence of pressure gradients and body forces, Cauchy's equation of motion for this flow geometry is

$$\frac{\partial u}{\partial t} = \frac{1}{\rho} \frac{\partial}{\partial y} [\tau_{xy}], \quad (1)$$

where τ_{xy} is the shear stress. The variation of density, ρ , across the interface is expected to be small and is neglected. By assuming a material flow law such as the Herschel-Bulkley model [7],

$$\tau_{xy} = \tau_0 + C \left(\frac{\partial u}{\partial y} \right)^m, \quad (2)$$

where τ_0 and C are strength parameters, m is strain-rate sensitivity ($0 \leq m \leq 1$), and $\frac{\partial u}{\partial y}$ is shear strain rate. The PDE (1) can be transformed into an ordinary differential equation (ODE) in one variable, by making an appropriate substitution such as

$$\lambda = yt^\alpha, \quad \text{where } \alpha = -(1+m)^{-1}. \quad (3)$$

Using Eqs. (1)–(3) and the chain rule, one gets

$$\lambda \frac{\partial u}{\partial \lambda} = t^{\alpha(m+1)+1} \left(\frac{C}{\rho \alpha} \right) \frac{\partial}{\partial \lambda} \left[\left(\frac{\partial u}{\partial \lambda} \right)^m \right]. \quad (4)$$

By substituting the value of α from Eq. (3), the t terms in Eq. (4) can be eliminated, giving an ODE in λ , which on simplification gives

$$\lambda \left(\frac{du}{d\lambda} \right)^{2-m} = - \left(\frac{Cm(1+m)}{\rho} \right) \frac{d^2 u}{d\lambda^2}. \quad (5)$$

Integrating Eq. (5) twice, we obtain

$$u = \left(\frac{Cm(1+m)}{(1-m)\rho K_1} \right)^{1/(1-m)} \times \lambda \left[{}_2F_1 \left(\frac{1}{2}, \frac{1}{1-m} \middle| \frac{3}{2} \middle| \frac{-\lambda^2}{2K_1} \right) \right] + K_2. \quad (6)$$

${}_2F_1(a, b|c|w)$ is a Gauss hypergeometric function with parameters a , b , c , and w . K_1 and K_2 are constants of integration to be evaluated using the BCs. From the BC at $y = 0$, $K_2 = 0$. A linear transformation [8],

$${}_2F_1(a, b|c|w) = (1-w)^{-a} {}_2F_1 \left(a, c-b|c| \frac{w}{w-1} \right), \quad (7)$$

may be applied to Eq. (6) such that

$$u = \left(\frac{Cm(1+m)}{(1-m)\rho K_1} \right)^{1/(1-m)} \sqrt{2K_1} \lambda \times \left[{}_2F_1 \left(\frac{1}{2}, \frac{1-3m}{2(1-m)} \middle| \frac{3}{2} \middle| \lambda^2 \right) \right], \quad (8)$$

where $\lambda \equiv \lambda(2K_1 + \lambda^2)^{-1/2}$. At $y = \pm\infty$, $yt^\alpha = \lambda = \pm\infty$ and $\lambda = \pm 1$, and it can be shown [8] that

$$\lim_{\lambda \rightarrow 1} \lambda \left[{}_2F_1 \left(\frac{1}{2}, \frac{1-3m}{2(1-m)} \middle| \frac{3}{2} \middle| \lambda^2 \right) \right] = \frac{\Gamma(\frac{3}{2})\Gamma(\frac{m+1}{2(1-m)})}{\Gamma(\frac{1}{1-m})} \equiv \Theta(m), \quad (9)$$

where $\Gamma(\beta)$ is the gamma function of variable, β . Combining Eqs. (8) and (9) and the BC at $y = \pm\infty$, gives

$$K_1 = \left[\frac{Cm(1+m)}{\rho(1-m)} \left(\frac{\sqrt{2} \cdot \Theta(m)}{U} \right)^{(1-m)} \right]^{2/(m+1)}. \quad (10)$$

Combining Eqs. (9) and (10) yields the velocity profile

$$u_n \equiv \frac{u}{U} = \frac{1}{\Theta(m)} \lambda \left[{}_2F_1 \left(\frac{1}{2}, \frac{1-3m}{2(1-m)} \middle| \frac{3}{2} \middle| \lambda^2 \right) \right]. \quad (11)$$

Equation (11) represents the normalized velocity u_n as a function of “normalized λ ,” λ . The hypergeometric function is a series solution and the exact functional form depends on m , the strain-rate sensitivity of the material, which in turn depends on temperature and strain rate. For many metals, $m \leq 0.2$ [9]. For plastics and amorphous materials, m is typically close to unity [10,11]. For special values of m , the hypergeometric function assumes simpler functional forms. The specific functional form in Newtonian fluids and in ideal (Bingham) plastic flow, for which $m = 1$, is the error function solution, and this result is well known in the fluid mechanics literature. For crystalline solids with smaller m values, specific functional forms include $u = \frac{2U}{\pi} \arctan(\frac{yt^{-1}}{\sqrt{2K_1}})$ for $m = 0$ and $u = Uyt^{-3/4}(2K_1 + y^2t^{-3/2})^{-1/2}$ for $m = 1/3$. Normalized velocity profiles from Eq. (11) are shown in Fig. 2(a) for selected m values in the range $0 \leq m \leq 1$. The profiles in Fig. 2(a) do not correspond to actual velocity profiles owing to the present normalization scheme wherein $y = \pm\infty$ in real length units corresponds to $\lambda = \pm 1$ in the normalized scale. The normalized velocity profile for OFHC copper, for which flow parameters are known [12], is indicated in Fig. 2(b) for different sliding velocities. The strain-rate profile, $\frac{du}{dy}$, is indicated in Fig. 3 at different times and for different sliding velocities. The spreading of the deformed zone is evident in Fig. 3(a). If m were to stay constant during the course of sliding, the developing flow during sliding would be “self-preserving” such that the velocity profile at any time would retain the same functional form while merely changing transverse length scales. It is interesting to note that the results suggest that the rate of spreading of the deformed zone is determined by α and K_1 . If a characteristic width, y^* , is defined for the extent of plastic deformation, then if $m = 1$,

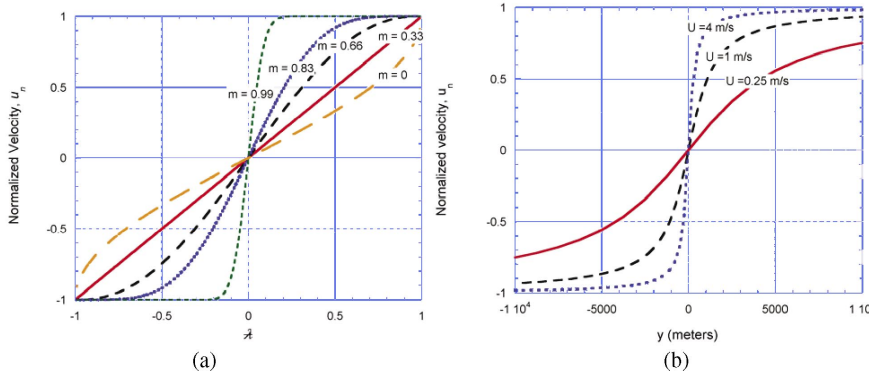


FIG. 2 (color online). (a) Normalized velocity profiles as functions of λ for selected values of m . Profile shapes are due to the normalization scheme; the linear dependence for $m = 0.33$ is also a consequence of this. (b) Normalized velocity profiles for different sliding velocities ($t = 1$ s). Flow parameters for OFHC copper [12]: $C = 231 \text{ MPa} \cdot \text{s}^m$ and $m = 0.0153$. Note that the large length scales result from the infinite system size.

$y^* \propto t^{1/2}$. This is consistent with a result from MD simulations of sliding of a simple amorphous material [13]. However, if $m = 0$, as is almost the case for many metals, then $y^* \propto t$. As seen in Figs. 2(b) and 3(b) the model suggests that increasing the sliding velocity U results in a smaller value of K_1 , and this leads to localization of deformation. By interrupting sliding experiments at different times and by characterizing the width of the deformed zone one could test these predictions.

Displacement and strain profiles may be obtained by integrating the velocity and strain-rate profiles, respectively, over time. Preliminary results suggest that the form of measured displacement profiles previously characterized in longitudinal cross sections of worn samples [14] compare favorably with the predictions made here. The utility of strain-rate profiles extends to the prediction of transient friction behavior if friction arises mainly from plastic dissipation. This depends on both the strain-rate profile and the associated shear stresses, which in turn depend on shear strain rate via Eq. (2). A transient strain-rate thus leads to transient friction behavior. The friction force drops with time for $0 \leq m \leq 1$, the time dependence depending on the exact value of m . Experimental observations of similar transient friction behavior lend support to the approach taken here.

In real friction experiments, however, it is often observed that the friction force ceases to drop continuously and approaches a “steady-state” value. At steady state, the rate of dissipation and the velocity profile are time invariant. In ideal homogeneous fluids that retain their properties over the course of sliding, such steady state is impossible. However, a steady state is possible in real materials since they tend to develop property gradients for thermal and/or structural reasons. Plastic deformation, being a dissipative process, leads to temperature increase. This, in turn, leads to an increase in the strain-rate sensitivity, thermal softening of material adjacent to the sliding interface and localization of deformation. A balance between localization and spreading leads to steady-state velocity and temperature profiles. The evolution of the velocity profile thus depends on the evolution of temperature-dependent material properties.

Besides temperature, strain hardening (or softening) during sliding is another probable cause of property gra-

dients. Unlike perfect fluids, the flow stress in most solids is not only a function of strain rate, but also of strain and strain path. Plastic strain is largest close to the sliding interface and continuously decreases away from the interface. In metals, this is structurally manifested in the form of a nanoscale “tribolayer” near the interface and deformation substructure, with a coarsening size scale, away from the interface [1,2]. Amorphous materials are structurally characterized by decreased density associated with increased free volume closer to the interface [13,15]. Such gradients in structure lead to gradients in flow properties. Higher strains in metals are typically characterized by smaller subgrains and higher flow stresses. In addition, finer substructures usually deform with larger strain-rate sensitivities [16–18].

The symmetric solutions presented here were derived for self-mated sliding pairs. When two dissimilar materials are brought into contact, the resulting profiles are expected to be asymmetric. In such cases, the density difference across the interface cannot be neglected. Moreover, mixing of components across the interface has been observed and simulated in real sliding situations [13,19], and this could contribute to spatial and temporal variations of material properties. In this Letter, development of property profiles is neglected and no attempt is made to predict steady-state velocity profiles. However, nontrivial solutions ought to exist since velocity profiles depend on structure and temperature, which are state variables.

This model ignores the presence of asperities by assuming flat sliding interfaces. Also, it was implicitly assumed that the entire material is free to deform plastically, whereas most solids have well defined elastic limits below which they do not undergo permanent deformation. Dependence of yield stress on strain and strain path, incorporation of property profiles, finite boundary conditions, and the contribution of normal load to the yield criterion are among the topics worth addressing in subsequent model refinements. For such complicated cases, the use of numerical techniques will be more efficient and perhaps necessary. However, the exact solution derived here retains the advantage of serving as a benchmark for testing the convergence of numerical solutions. It also provides insights into the relationship between flow and

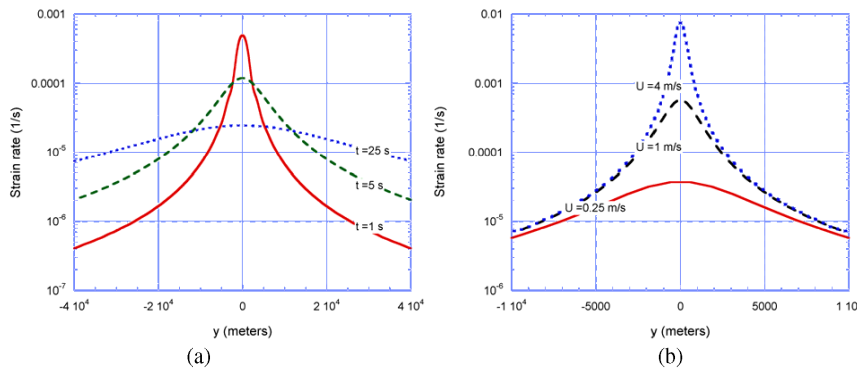


FIG. 3 (color online). (a) Strain-rate profiles reveal spreading of deformation with time ($U = 1\text{ m/s}$); (b) strain-rate profiles at different sliding velocities show greater localization at higher sliding velocities ($t = 1\text{ s}$). Flow parameters for OFHC copper as in Fig. 2 [12].

material parameters, many of which are nonintuitive. The exact solution offers a clear and isolated way of testing the dependency of friction and flow behavior on material properties.

It is suggested that the applicability of this technique for determining strain-rate and strain profiles is not restricted to tribology. The understanding of analogous shearing processes such as explosive welding and the formation of shear bands could be enhanced by this approach. The microstructure of the weld interface due to explosive welding and that within shear bands is characterized by the formation of ultrafine crystalline material [20], a feature that is also observed in the microstructure adjacent to sliding interfaces [1,2]. Furthermore, recent MD simulations show that vorticity plays an important role in the formation of this tribolayer during sliding [4]. Waves and vortices have also been observed in explosively welded interfaces [21]. At much larger size scales, the development of fine-grained mylonite where tectonic plates interact may be related [22]. These observations suggest that, despite diversity in size scale and mechanistic details of deformation, the nature of flow in these shear phenomena is broadly similar. Thus, the continuum method adopted in this study may have wide-ranging applications.

In summary, an equation of motion was successfully applied to the problem of determining velocity profiles developed during sliding of materials. The continuum technique invoked momentum balance and generic material flow laws without delving into detailed deformation mechanisms. It was found that the shape of the velocity profile is determined by the strain-rate sensitivity, while the spatial extent of deformation is determined by strain-rate sensitivity, strength parameters, and sliding velocity. It was also found that these parameters control transient friction and the rate of spreading of deformation. Knowledge of velocity and strain-rate profiles is expected to enhance the understanding of sliding friction mechanisms and associated microstructures.

The authors acknowledge Dr. J. Hammerberg at Los Alamos National Laboratories, Dr. A.T. Conlisk, Dr. J. Li, and Dr. Y.Z. Wang at The Ohio State University, Dr. J.-H. Wu at the University of Arkansas, and Dr. M.L. Falk at the University of Michigan for their ideas, criti-

cism, and encouragement. This research was sponsored by the National Nuclear Security Administration under the Stewardship Science Academic Alliances program through DOE Grant No. DE-FG03-03NA0006.

-
- [1] D. A. Rigney, *Wear* **245**, 1 (2000).
 - [2] D. A. Hughes and N. Hansen, *Phys. Rev. Lett.* **87**, 135503 (2001).
 - [3] J.-H. Wu *et al.*, *Wear* **259**, 744 (2005).
 - [4] S. Karthikeyan, J.-H. Wu, and D. A. Rigney, in *Proceedings of the Symposium on Nanoscale Materials and Modeling*, edited by P. M. Anderson *et al.* (MRS, San Francisco, 2004), Vol. 821, p. 9.6.1.
 - [5] W. Kelvin, *Philos. Mag.* **42**, 362 (1871).
 - [6] H. von Helmholtz, *Philos. Mag.* **36**, 337 (1868).
 - [7] W. Herschel and R. Bulkley, *Kolloid Z. Z. Polym.* **39**, 291 (1926).
 - [8] F. Oberhettinger, in *Handbook of Mathematical Functions*, edited by M. Abramovitz and I. A. Stegun (Dover, New York, 1972), p. 556.
 - [9] G. E. Dieter, *Mechanical Metallurgy* (McGraw-Hill, London, 1988).
 - [10] C. A. Schuh, A. C. Lund, and T. G. Nieh, *Acta Mater.* **52**, 5879 (2004).
 - [11] T. A. Osswald and G. Menges, *Materials Science of Polymers for Engineers* (Hanser/Gardner Publications, Inc., Cincinnati, 1995).
 - [12] P. S. Follansbee and U. F. Kocks, *Acta Metall.* **36**, 81 (1988).
 - [13] X. Y. Fu *et al.*, *Wear* **250**, 420 (2001).
 - [14] D. A. Rigney *et al.*, *Mater. Sci. Eng. A* **81**, 409 (1986).
 - [15] X. Y. Fu *et al.*, *Wear* **250**, 409 (2001).
 - [16] R. Z. Valiev *et al.*, *J. Mater. Res.* **17**, 5 (2002).
 - [17] H. S. Kim and Y. Estrin, *Acta Mater.* **53**, 765 (2005).
 - [18] K. S. Kumar, H. van Swygenhoven, and S. Suresh, *Acta Mater.* **51**, 5743 (2003).
 - [19] J. E. Hammerberg *et al.*, *Metall. Mater. Trans. A* **35**, 2741 (2004).
 - [20] M. A. Meyers *et al.*, *Mater. Sci. Eng. A* **317**, 204 (2001).
 - [21] M. Hammerschmidt and H. Kreye, in *Shock Waves and High-Strain Rate Phenomena in Metals*, edited by M. A. Meyers and L. E. Murr (Plenum Press, New York, 1981).
 - [22] T. A. Little, R. J. Holcombe, and B. R. Ilg, *J. Struct. Geol.* **24**, 193 (2002).